

Seismic Potential and Feasibility of Harvesting and Storing Earthquake Energy for Iran

Mansoureh Rezaeemanesh^{a}, Mohammad Hematibahar^b, Mohammad Rezaeemanesh^c, Ali Alibazi^a, Makhmud Kharun^d*

^a *Master of Science, Earthquake Engineering, Faculty of Civil, Water and Environmental Engineering, Shahid Beheshti University, Tehran, Iran*

^b *Master of Science, Structural Engineering, Department of Architecture, Restoration and Design, RUDN University, Moscow, Russia*

^c *Master of Science, Mechanical Engineering, Islamic Azad University, Semnan Branch, Semnan, Iran*

^d *Associate professor, Department of Reinforced Concrete and Stone Structures, Moscow State University of Civil Engineering, Moscow, Russia*

* *Corresponding author e-mail: mrezaeemanesh1994@gmail.com*

Abstract

Iran is one of the most seismically active regions in the world. With each earthquake, a relatively large amount of kinetic energy is released on the surface of the earth. In the history of Iran, the occurrence of any earthquake has always been recorded as a major hazard. Considering the importance of using new energies and reducing the use of fossil fuels in seismically active regions such as Iran, the energy from earthquakes can be used as a suitable opportunity to provide alternative energy. This requires that the feasibility of harvesting and storing earthquake energy be examined first. Therefore, in this paper, the released energy of earthquakes that have occurred in Iran since 1974 was examined separately for each seismic zone in Iran and also for each decade in which the earthquake occurred, and finally, the energy released in the earthquake was compared with the required electrical energy. As a general conclusion, it can be said that Iran has a great potential for harvesting energy theoretically, but it is not currently justified from a practical and economic perspective.

Keywords: Earthquake energy; Vibrating piezoelectric, Earthquake harvesting; Ground motion.

Introduction

Earthquakes, while destructive, release substantial magnitude-dependent energy that offers potential for future energy harvesting [1–4]. Thus, evaluating released energy relative to earthquake magnitude remains an important research topic. Understanding earthquake energy release depends on multiple parameters. Various methods have been proposed, such as Mattesini's estimates of total released energy showing deep earthquakes can produce up to six times more rupture energy than

radiated energy [5,6]. Ommi and Smirnov [7] also introduced a method identifying energy release patterns before the mainshock. Overall, different approaches exist for defining earthquake energy release. Studies show that earthquake potential energy comprises elastic, strain, and gravitational components, along with radiant, fracture, and thermal energies [8]. Elastic and radiant energies are influenced by fault heterogeneity [8,9], and less than 20% of the total energy is radiated as seismic waves. Understanding how energy is partitioned within the fault zone is essential for earthquake mechanics; the energy budget is typically expressed as work density per fault area [10,11]. Most of this budget is associated with fracture processes [12–14]. Seismic energy (E) can be simply estimated from earthquake magnitude (M) using the relation $\log(E=1.5M + 11)$ [15]. Radiated energy reflects fault dynamics, and the scaled energy $e = ER/M_0$ is used to assess the dependence of seismic energy on moment [16,17]. Ide and Beroza showed that energy estimates for small earthquakes are underestimated due to instrumental bandwidth limits [18–20]. Various studies have proposed methods to estimate earthquake energy. Ommi et al. [7] predicted magnitude and failure time from preseismic energy release in the Fin doublet. Toffol et al. [21] estimated ~ 13 MJ/m² of released energy from shocked garnet, mainly from heat, surface energy, and lattice distortion. Kato [22] reported rupture energies ranging from 0.1–1 MJ/m² for Mw 4.8 Nankai events to ~ 10 MJ/m² for the Mw 9 Tohoku-oki earthquake, showing fracture energy increases with magnitude. Several studies have examined patterns of earthquake energy release. Lin et al. [23] showed that 98% of earthquakes occur shallower than 100 km, with 49%, 7%, and 12% of total energy released at 0–20 km, 20–40 km, and 40–60 km depths, respectively, indicating dominant activity in the brittle upper crust. Varga et al. [24] found that 60–76% of earthquake energy dissipates within the upper 50 km, while only about 20% is released throughout the deeper subduction zone (50–550 km). Miao and A. Langston [25] studied the released energy around the U.S.A, they found that releasing energy in the central of United State rather than other places is lower and the north of United State had the maximum amount of energy releasing. While the most releasing earthquake energy in Iran happen in the South, East and sometimes central. Telesca et al. [26] done Multifractal Detrended Fluctuation Analysis (MF-DFA) for El Hierro volcano (Canary Islands). They found that released energy is more than 8 GJ considering by GR law. It should be considered that the short- and medium-periods happening earthquake is 1 s and 5 s. In addition, many researchers try to harvest earthquake energy in different ways. As an example, R. Kivi et al. [27] analyzed injection-induced seismicity through "Enhanced Geothermal Systems (EGS)". They understand that injection-induced seismicity can be prepared and safely unlocked the enormous potential of clean and sustainable geothermal energy. In this type of energy harvesting, the fault is controlled to form an earthquake and the geothermal energy from the broken rocks is stimulated at the moment of the earthquake. Although most of the seismicity caused by EGS has small magnitudes [28], it can contribute to earthquake energy harvesting. In another example, Díaz-Mora and González-Fallas [29] attempted to convert seismic waves into electricity by converting the kinetic energy of earthquakes into potential energy. Satyanarayana et al. [30] have researched the conversion of earthquake vibrations into electricity through the servo-electric vibration sensor in the vibration table. Iran as a potential region for the occurrence of earthquakes with high magnitudes and having many faults can extract a large amount of energy from earthquakes [31–33]. For example, Talebi et al. [34] has mapped the faults and probability of earthquake in the east of Iran. Their goal was to make the connection between studies of earthquake activity and buildings resistant to impending earthquakes. In another study, Gutierrez et al. [35] investigating the geotectonic phenomenon in the Zagros Mountain range, south of Iran. They analyzed strike-slip salt diapir systems and the relationship of strike-slip faults. They found that the Kareh Bas fault system, despite its fragmentation and even if the ruptures are confined to the overlying salt mantle, is capable of generating large earthquakes of Mw 6.5–7. As far as the studies conducted indicate that due to the occurrence of large and small earthquakes, Iran has the ability to be rich in clean energy caused by earthquakes. The purpose of this study is to measure the amount of energy emitted from all earthquakes in Iran based on magnitude unit. This research was done with the aim of obtaining Iran's annual energy budget from earthquakes and related formulas. This re-

search can be useful as a basis or a step for extracting and collecting earthquake energy in Iran in the future.

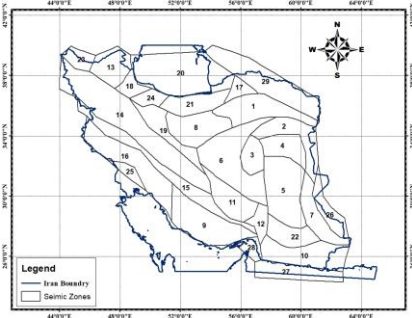


Fig. 1. Seismic Zone (SZ) of Iran [38].

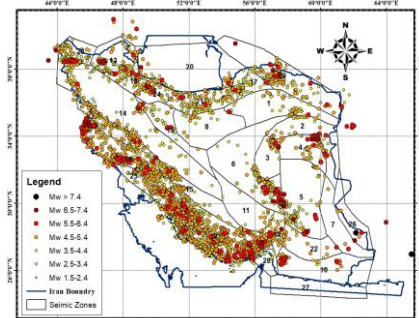


Fig. 2. The earthquakes according to Magnitudes and SZ in the current study.

2. Methodology

2.1. Methodology of Seismic Potential

Iran, located in the active Alpine-Himalayan belt, experiences many earthquakes [36]. Notable examples include the Kobe earthquake (1995) in Japan and the Bam earthquake (2003) in Iran [37]. Due to its wide geographical and geological diversity, this study investigates the seismic potential of different Iranian zones. Karimiparidari et al. [38] reported over 29 Seismic Zones (SZ) in Iran (Fig. 1), and earthquake magnitudes (M_w) across these zones were analyzed using ArcGIS (Fig. 2).

2.2. Database

This study analyzed the number of 10899 earthquake records with M_w between 1.9 and 7.7 with distance from source from 1 km to 600 km to find the discovery the energy. These records have been gathered from Road, Housing & Urban Development Research Center website [39]. Table 1 illustrates the records and specific details, Fig. 3 illustrates the data location and, moreover Fig. 4 illustrates of distribution of earthquake records.

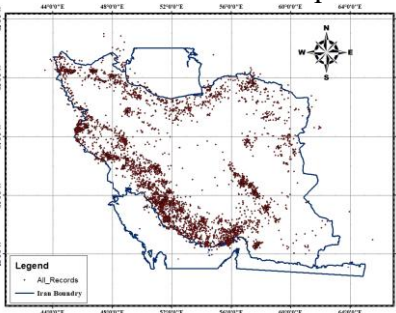


Fig. 3. The earthquakes events in the current study.

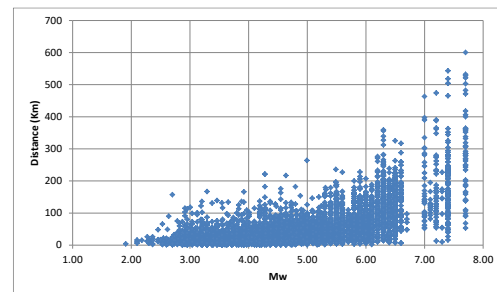


Fig. 4. Data distribution of earthquake records.

Table 1. Some records in this investigation.

Station Name	Record Num.	Date	PGA (cm/s/s)	Lat.	Long.	Distance (Km)	Station Code	VS30	M_w
Minab*	1007	7/03/1975 7:04	27	27.47	56.44	72	MIB-A	453	6.10
Makoo*	1046/02	24/11/1976 12:36	72	39.24	44.27	22	MAK-A	441	5.44
Naqan*	1061/04	26/04/1977 17:34	19	32.78	48.6	221	NGN2-A	700	4.28
Vandik*	1065/03	19/03/1977 3:29	162	33.82	59.36	12	VAK-A	658	4.73
Tabas*	1103/03	17/01/1979 3:29	115	33.74	57.09	24	TBS-A	650	5.09

2.3. Calculating Energy

Fault movement causes displacement and releases energy, with earthquake magnitudes following an exponential distribution. Converting magnitude to seismic energy follows the Gutenberg-Richter (GR) law [40], which can be calculated as described in [41]. In this study, the GR relation is applied using the following equation [42,43]:

$$\log E = 11.8 + 1.5M_w \quad (1)$$

Here, E is energy and M_w is earthquake magnitude. Many studies have used the GR equation to estimate earthquake energy; for example, Maine and Al Kindy [44,45]. Pisarenko and Sornette [46]

applied statistical tests using the Generalized Pareto Distribution (GPD). About 60% of released energy dissipates within 50 km, while 6% occurs in a narrow interval at 550–680 km depth [24]. Released energy is divided into radiated, fracture, and thermal components [8].

2.4. Current Study Methods

This study analyzed earthquakes by magnitude and date. Magnitudes were divided into <4.5 Mw and ≥ 4.5 Mw, and released energy was reported per decade (Fig. 5). Records from 29 SZ were applied to the GR equation, and results separated by magnitude. Magnitudes ≥ 4.5 Mw have significant building impact, while <4.5 Mw are generally harmless [47].

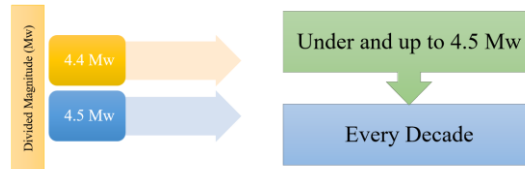


Fig. 5. The scheme of the current study.

3. Results

3.1. Under 4.5 Mw Earthquakes

Higher-magnitude earthquakes release more energy. For example, a 3.65 Mw earthquake releases 5,282 J, while a 4.37 Mw event releases over 62,687 J (Fig. 6). Earthquakes below 3 Mw have negligible energy release, but energy rises sharply above 3 Mw (e.g., 3.6 Mw \rightarrow 4,402 J; 4.3 Mw \rightarrow 49,396 J) (Fig. 6). Post-1974, more records increased observed values. Decadal energy sums (Table 2, Fig. 7) show 2010–2020 released >5.795 MJ, 2000–2010 >3.353 MJ, and 2020–2024 >1.660 MJ. Earthquake source distance also varies, mostly 167–182 km, except 1974–1980 with >221 km (Fig. 7b).

Table 2. The released energy by each year.

Year Interval	Sum J (Kwatt.Hr)	Min Mw	Max Mw	Min Distance (Km)	Max Distance (Km)
1974-1980	45498	3.65	4.46	11.00	221.00
1980-1990	29767	3.83	4.46	5.00	98.00
1990-2000	674938	3.21	4.46	0.00	182.00
2000-2010	3353082	1.91	4.48	1.00	166.00
2010-2020	5795128	2.36	4.48	0.00	167.00
2020-2024	1660156	2.50	4.48	0.00	167.00

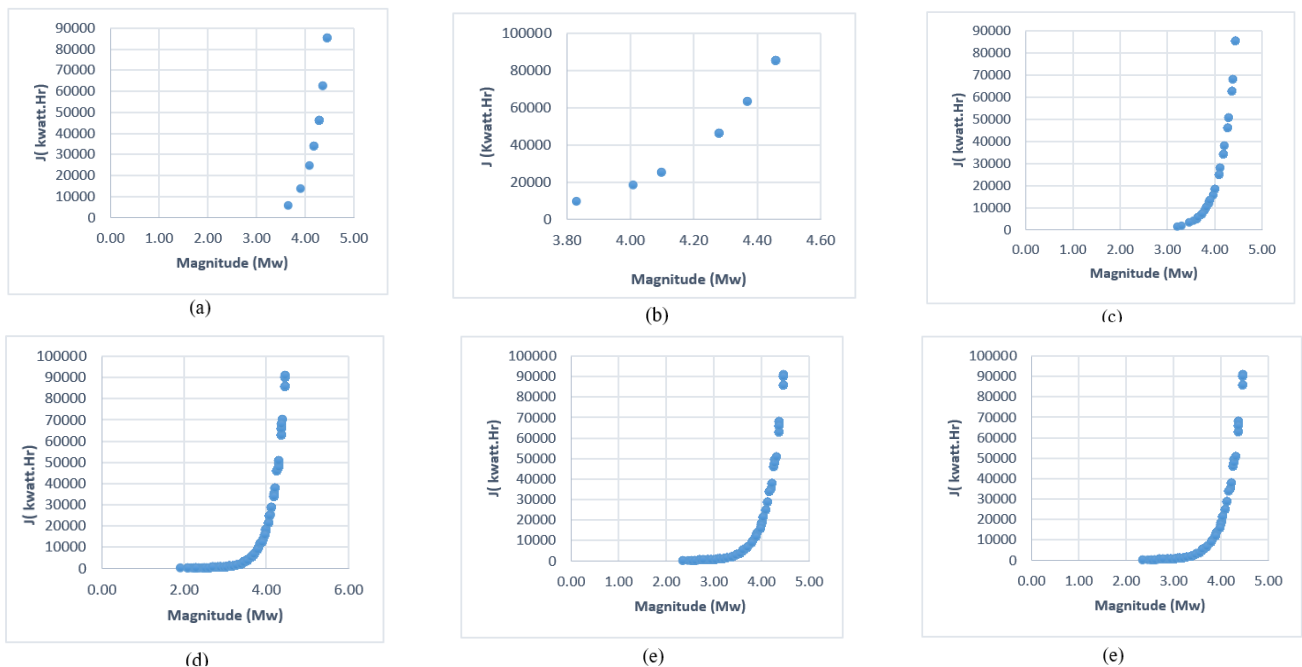


Fig. 6. Results of under 4.5 Mw per decade. (a) 1974-1979; (b) 1980-1989, (c) 1990- 1999, (d) 2000-2009 (e) 2010-2019.

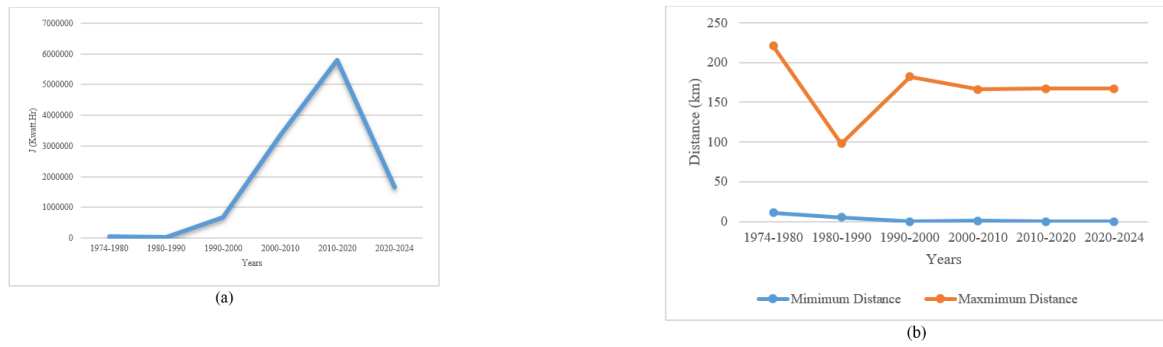


Fig. 7. Details of releasing energy. (a) Sum of energy in different decades, (b) Maximum and minimum distance of source earthquake.

3.2. Up to 4.5 Mw Earthquakes

This section examines earthquakes with $M_w > 4.5$. Table 3 and Fig. 8 show that higher magnitudes release more energy, posing greater risks to structures and cities (e.g., 4.64 Mw \rightarrow 0.158 MJ; 6.50 Mw \rightarrow 9.856 MJ) (Fig. 8). Between 2000 and 2010, the total released energy could have reached >595 GJ (Fig. 9a, Table 3). Earthquake source distances ranged from 0–7 km up to >600 km (Fig. 9b).

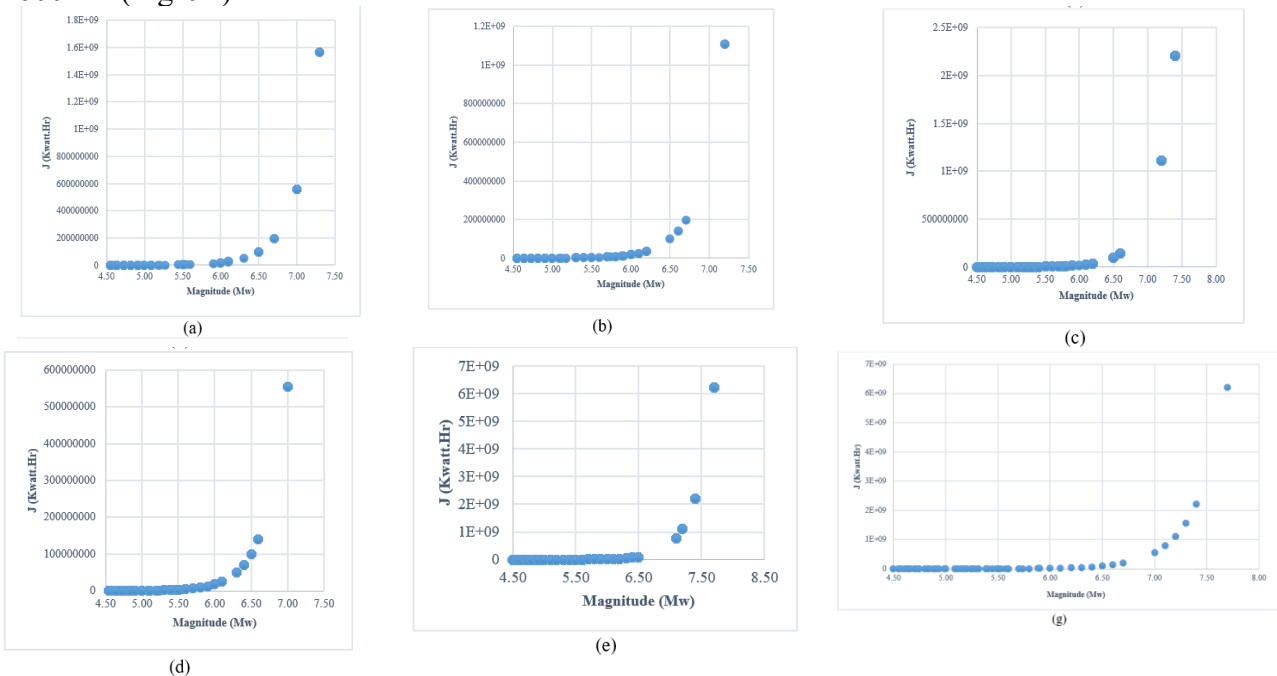


Fig. 8. Results of up to 4.5 Mw per decade. (a) 1974-1979; (b) 1980-1989, (c) 1990-1999, (d) 2000-2009 (e) 2010-2019.

Table 3. The released energy by each year.

Year Interval	Sum J (Kwatt.Hr)	Min Mw	Max Mw	Min Depth	Max Depth
1974-1980	2.85E+10	4.60	7.00	7.00	132.00
1980-1990	1.11E+10	4.64	5.00	7.00	73.00
1990-2000	8.83E+10	4.55	7.40	2.00	236.00
2000-2010	5.95E+11	4.50	7.40	0.00	474.00
2010-2020	3.14E+10	4.50	7.70	1.00	600.00
2020-2024	4.47E+09	4.55	7.70	1.00	600.00

3.3. Results of the Earthquake Energy Considering Seismic Zone

However, results of this study divided by two factors (the earthquakes bellow 4.5 Mw and more than 4.5 Mw), while Fig 10. illustrates energy releasing for all magnitudes and Table 4. shows the released energy for all SZ. Fig. 10. shows that the pattern release energy is higher during high-

magnitude earthquakes, but the cumulative energy released is more effective than one or two high-magnitude earthquakes.

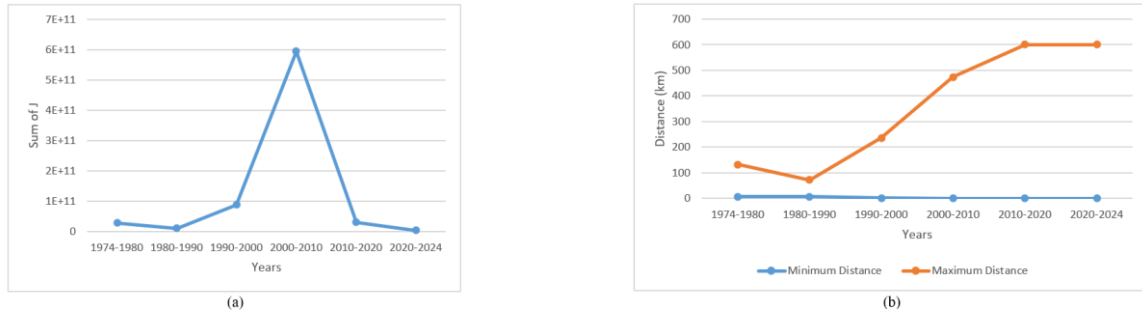


Fig. 9. Details of releasing energy. (a) Sum of energy in different decades, (b) Maximum and minimum distance to source of earthquake.

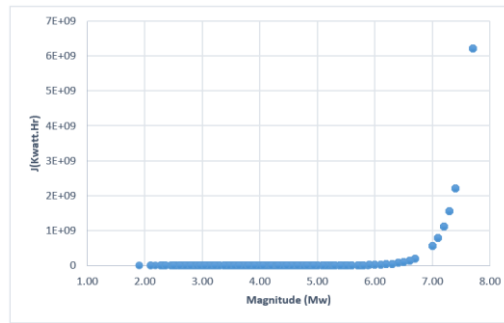


Fig. 10. All releasing energy per years.

Zone 26 releases the most energy due to high-magnitude earthquakes (4.3–7.7 Mw) but is unsuitable for energy harvesting because of low earthquake frequency and high damage risk. Zone 8 has minimal energy release and few earthquakes, making it unsuitable. Zone 16 in the Zagros region has the highest number of earthquakes (2.6–7.4 Mw), offering good energy potential but also risk to equipment. Zone 9 is suitable for earthquake energy absorption, with many events up to 6.7 Mw.

Table 4. Released energy for all seismic zones.

Zone Number	Number of earthquakes	Min Mw	Max Mw	Min Distance (Km)	Max Distance (Km)	Sum of Energy (MJ) (Kwatt.Hr)
1	118	2.8	5.8	4	167	168.8
2	64	2.9	6.1	5	116	93.8
3	49	2.8	6.0	2	96	63.7
4	194	3.0	7.3	2	474	56912.8
5	327	2.1	7.2	1	288	15898.7
6	688	2.3	7.2	1	317	6019.6
7	10	4.4	6.0	16	108	74.4
8	26	3.2	5.3	3	115	4.2
9	1876	2.7	6.7	1	218	5818.3
10	101	3.3	6.2	5	112	350.0
11	31	3.4	5.4	3	131	21.7
12	101	3.2	6.6	5	249	2685.4
13	1469	2.5	6.5	0	217	15457.0
14	581	1.9	6.5	1	325	8027.8
15	699	2.4	7.4	0	174	3282.3
16	2030	2.6	7.4	0	543	190118.1
17	39	3.3	5.5	3	97	28.4
18	181	2.8	7.4	1	259	50892.1
19	135	2.9	6.2	4	162	358.8
20	229	2.9	6.5	3	162	366.5
21	619	2.7	6.3	1	359	7553.2
22	33	3.5	5.5	8	150	25.3
23	133	2.9	5.7	3	118	90.8
24	112	3.0	5.7	2	93	42.3
25	77	3.0	5.8	4	217	98.9
26	57	4.3	7.7	16	600	280061.8
27	-	-	-	-	-	-
28	162	2.9	6.1	2.0	172.0	636.3
29	343	2.6	7.0	1.0	463.0	9031.2
Min	10	1.9	5.3	0.0	93.0	4.2
Max	2030	4.4	7.7	16.0	600.0	280061.8

3.4. Consuming Energy

From 2000 to 2008, earthquake energy in Iran often exceeded electricity production [48], with Mw >4.5 events contributing most [49]. Between 2003–2013, released energy surpassed consumption, showing potential to improve energy balance [50]. However, high costs, unpredictability, and risks make harnessing this energy currently impractical, though it remains a promising future renewable source alongside solar and wind.

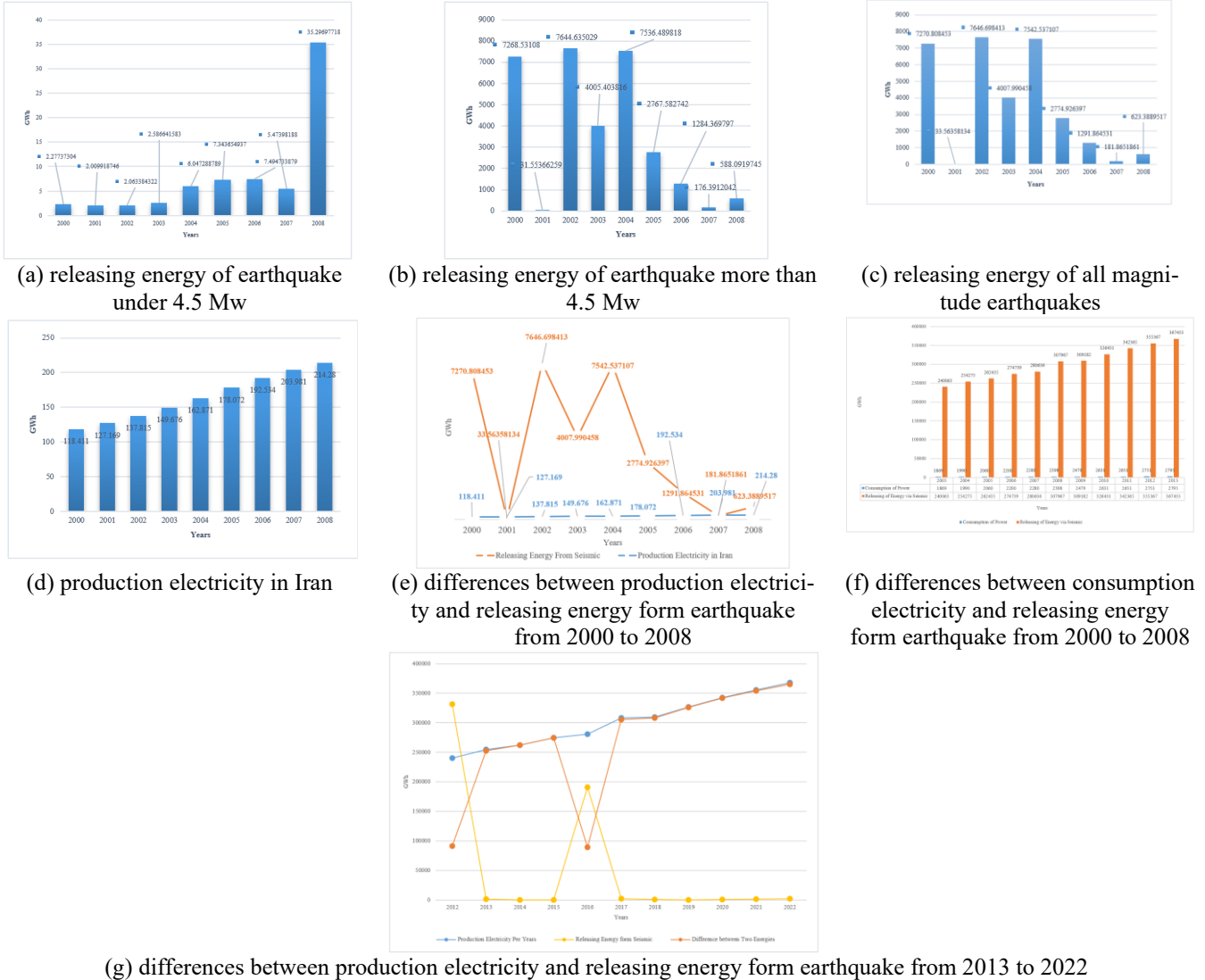


Fig. 11. investigating the production electricity, consumption electricity and releasing energy of earthquake in 2000-2008 [51]

4. Discussion

Theoretically, the energy released in an earthquake is very significant and impressive, but its practical aspect also needs to be examined. From this practical aspect, the idea was investigated by choosing an earthquake with 4.3 Mw and also by choosing an existing piezoelectric.

Considering the information on the earthquake with 4.3 Mw, frequency equal to 47.73 Hz and PGA equal to 0.42g m/sec², the electrical energy generated by the earthquake can be calculated

The Murata company's vibrating piezoelectric catalog [52] was used to calculate the energy from earthquake vibration (Fig. 12). According to the above diagram, for a 4.3 Mw earthquake, about 50mv of voltage will be generated. $V=50\text{mv}$

The piezoelectric sensor performed like a capacitor. Using the charging amplifier circuit, the energy generated and stored in it is obtained from the following equation:

$$E = \frac{1}{2} CV^2$$

Where, E is the energy stored in the capacitor, C is the capacitance of the capacitor and V is the voltage applied to the capacitor. Considering the selection of the PKS1-4A1 vibrating piezoelectric, the capacitance of the capacitor will be C=10000 PF. Keep in mind that the cross-sectional area of the above piezoelectric sensor is about 7 (cm)².

$$C = 10000 \times 10^{-12} \text{ F}$$

Energy calculation:

$$E = \frac{1}{2} CV^2$$

We already have: V=50mv and assuming that the maximum voltage can be obtained from such a sensor:

$$V = 5 \text{ v}$$

The amount of electrical energy per piezoelectric number will be as follows:

$$E = \frac{1}{2} \times 10000 \times 10^{-12} \times 5^2 = 1.25 \times 10^{-7} \text{ Jouls}$$

Covering a 1000 m × 1000 m area with sensors (~10⁹ sensors at \$40 each) would generate only 125 J during a 20 s earthquake, yielding ~7 W (1.4 A), which is negligible and economically unfeasible. In contrast, the same investment could fund a solar plant supplying daily electricity for five cities the size of Tehran. Thus, earthquake energy is currently impractical for electricity generation.

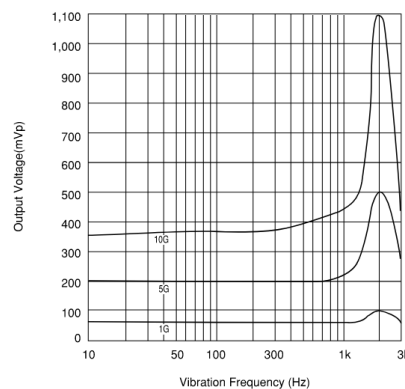


Fig. 12. Frequency Response is nearly flat at vibration frequencies up to 1kHz [52].

5. Conclusion

Iran's seismic activity offers theoretical potential for energy harvesting, but practical application is currently economically and technologically unfeasible due to the unpredictable nature of earthquakes. This study analyzed 10,899 Iranian earthquake records (1973–2024, Mw 1.9–7.7, distances 1–600 km) to assess seismic potential and energy harvesting feasibility. Records were divided into Mw <4.5 and Mw ≥4.5 due to structural impact. For potential harvesting, equipment must be placed in areas with continuous seismic activity for economic viability. Seismic zoning followed Karimi-Pridari et al. [38]. Zone 26 releases the most energy but is unsuitable due to infrequent, high-magnitude earthquakes. Zone 8 has low energy and activity, also unsuitable. Zone 16 (Zagros) has high earthquake frequency (2.6–7.4 Mw), offering potential but with risk. Zone 9 is a viable candidate for energy absorption, with many events up to 6.7 Mw. Operational assessment using piezoelectric systems shows earthquake energy is minimal and uneconomical. Low efficiency, high costs, and the sporadic nature of seismic events limit consistent energy generation, providing only a tiny fraction of Iran's electricity needs. Economic analysis shows harvesting earthquake energy is costlier than alternatives like solar or wind, which provide consistent, scalable energy better suited to Iran's infrastructure and policies. In conclusion, seismic energy use is scientifically interesting but currently impractical due to technological and economic limits. Future research should improve harvesting technologies, but prioritizing solar and wind investments is more effective for Iran's energy security and sustainability.

References

- [1] Pinzón N, Vargas CA. Global variation of seismic energy release with oceanic lithosphere age. *Sci Rep* 2021;11:601. <https://doi.org/10.1038/s41598-020-80475-y>.

- [2] Gudmundsson A. Elastic energy release in great earthquakes and eruptions. *Front Earth Sci* 2014;2. <https://doi.org/10.3389/feart.2014.00010>.
- [3] Kammer DS, McLaskey GC, Abercrombie RE, Ampuero J-P, Cattania C, Cocco M, et al. Earthquake energy dissipation in a fracture mechanics framework. *Nat Commun* 2024;15:4736. <https://doi.org/10.1038/s41467-024-47970-6>.
- [4] Mignan A, Karvounis D, Broccardo M, Wiemer S, Giardini D. Including seismic risk mitigation measures into the Levelized Cost Of Electricity in enhanced geothermal systems for optimal siting. *Appl Energy* 2019;238:831–50. <https://doi.org/10.1016/j.apenergy.2019.01.109>.
- [5] Fonsêca JAS, Ferreira JM, do Nascimento AF, Bezerra FHR, Lima Neto HC, de Menezes EAS. Intraplate earthquakes in the Potiguar Basin, Brazil: Evidence for superposition of local and regional stresses and implications for moderate-size earthquake occurrence. *J South Am Earth Sci* 2021;110:103370. <https://doi.org/10.1016/j.jsames.2021.103370>.
- [6] Mattesini M, Sánchez CL, Buforn E, Udías A, Valdés J de la S, Tavera H, et al. From an atomistic study of olivine under pressure to the understanding of the macroscopic energy release in earthquakes. *Geosystems and Geoenvironment* 2023;2:100108. <https://doi.org/10.1016/j.geogeo.2022.100108>.
- [7] Omni S, Smirnov VB. Seismicity patterns before the 2021 Fin (Iran) doublet earthquakes using the region-time-length and time-to-failure methods. *Earthq Sci* 2024;37:324–36. <https://doi.org/10.1016/j.eqs.2024.04.005>.
- [8] Kanamori H, Rivera L. Energy partitioning during an earthquake, 2006, p. 3–13. <https://doi.org/10.1029/170GM03>.
- [9] Rudnicki JW, Freund LB. On energy radiation from seismic sources. *Bull Seismol Soc Am* 1981;71:583–95. <https://doi.org/10.1785/BSSA0710030583>.
- [10] Bestmann M, Pennacchioni G, Nielsen S, Göken M, de Wall H. Deformation and ultrafine dynamic recrystallization of quartz in pseudotachylite-bearing brittle faults: A matter of a few seconds. *J Struct Geol* 2012;38:21–38. <https://doi.org/10.1016/j.jsg.2011.10.001>.
- [11] Papa S, Pennacchioni G, Angel RJ, Faccenda M. The fate of garnet during (deep-seated) coseismic frictional heating: The role of thermal shock. *Geology* 2018;46:471–4. <https://doi.org/10.1130/G40077.1>.
- [12] Beeler N, Kilgore B, McGarr A, Fletcher J, Evans J, Baker SR. Observed source parameters for dynamic rupture with non-uniform initial stress and relatively high fracture energy. *J Struct Geol* 2012;38:77–89. <https://doi.org/10.1016/j.jsg.2011.11.013>.
- [13] Nielsen S, Spagnuolo E, Violay M, Smith S, Di Toro G, Bistacchi A. G: Fracture energy, friction and dissipation in earthquakes. *J Seismol* 2016;20:1187–205. <https://doi.org/10.1007/s10950-016-9560-1>.
- [14] Guatteri M. What Can Strong-Motion Data Tell Us about Slip-Weakening Fault-Friction Laws? *Bull Seismol Soc Am* 2000;90:98–116. <https://doi.org/10.1785/0119990053>.
- [15] Gutenberg B. The energy of earthquakes. *Q J Geol Soc London* 1956;112:1–14. <https://doi.org/10.1144/GSL.JGS.1956.112.01-04.02>.
- [16] Kanamori H. Static and Dynamic Scaling Relations for Earthquakes and Their Implications for Rupture Speed and Stress Drop. *Bull Seismol Soc Am* 2004;94:314–9. <https://doi.org/10.1785/0120030159>.
- [17] Kanamori H, Heaton TH. Microscopic and macroscopic physics of earthquakes, 2000, p. 147–63. <https://doi.org/10.1029/GM120p0147>.
- [18] Ide S, Beroza GC. Does apparent stress vary with earthquake size? *Geophys Res Lett* 2001;28:3349–52. <https://doi.org/10.1029/2001GL013106>.
- [19] Izutani Y, Kanamori H. Scale-dependence of seismic energy-to-moment ratio for strike-slip earthquakes in Japan. *Geophys Res Lett* 2001;28:4007–10. <https://doi.org/10.1029/2001GL013402>.
- [20] Kanamori H. The energy release in great earthquakes. *J Geophys Res* 1977;82:2981–7. <https://doi.org/10.1029/JB082i020p02981>.
- [21] Toffol G, Pennacchioni G, Menegon L, Wallis D, Faccenda M, Camacho A, et al. On-fault earthquake energy density partitioning from shocked garnet in an exhumed seismic midcrustal fault. *Sci Adv* 2024;10. <https://doi.org/10.1126/sciadv.adi8533>.
- [22] Kato N. Fracture energies at the rupture nucleation points of large interplate earthquakes. *Earth Planet Sci Lett* 2012;353–354:190–7. <https://doi.org/10.1016/j.epsl.2012.08.015>.
- [23] Lin T-L, Mittal H, Wu C-F, Huang Y-H. Spatial distribution of radiated seismic energy from earthquakes in Taiwan and surrounding regions. *J Asian Earth Sci* 2020;204:104591. <https://doi.org/10.1016/j.jseaes.2020.104591>.
- [24] Varga P, Krumm F, Riguzzi F, Doglioni C, Süle B, Wang K, et al. Global pattern of earthquakes and seismic energy distributions: Insights for the mechanisms of plate tectonics. *Tectonophysics* 2012;530–531:80–6. <https://doi.org/10.1016/j.tecto.2011.10.014>.
- [25] Miao Q, Langston CA. Spatial Distribution of Earthquake Energy Release in the Central United States from a Global Point of View. *Seismol Res Lett* 2008;79:33–40. <https://doi.org/10.1785/gssrl.79.1.33>.
- [26] Telesca L, Lovallo M, Marti Molist J, López Moreno C, Abella Meléndez R. Multifractal investigation of continuous seismic signal recorded at El Hierro volcano (Canary Islands) during the 2011–2012 pre- and eruptive phases. *Tectonophysics* 2015;642:71–7. <https://doi.org/10.1016/j.tecto.2014.12.019>.
- [27] Kivi IR, Vilarrasa V, Kim K-I, Yoo H, Min K-B. On the role of poroelastic stressing and pore pressure diffusion in discrete fracture and fault system in triggering post-injection seismicity in enhanced geothermal systems. *Int J*

- Rock Mech Min Sci 2024;175:105673. <https://doi.org/10.1016/j.ijrmms.2024.105673>.
- [28] Evans KF, Zappone A, Kraft T, Deichmann N, Moia F. A survey of the induced seismic responses to fluid injection in geothermal and CO₂ reservoirs in Europe. *Geothermics* 2012;41:30–54. <https://doi.org/10.1016/j.geothermics.2011.08.002>.
- [29] Díaz-Mora F, González-Fallas A. Energy harvesting from seismic waves for electricity production. *E3S Web Conf* 2022;336:00035. <https://doi.org/10.1051/e3sconf/202233600035>.
- [30] Geetha L., Ashwini Satyanarayana ASA. Conversion of Earthquake Vibrations in to Electricity. *Tuijin Jishu/Journal Propuls Technol* 2023;44:842–54. <https://doi.org/10.52783/tjjpt.v44.i4.941>.
- [31] Raeesi M, Zarifi Z, Nilfouroushan F, Boroujeni SA, Tiampo K. Quantitative Analysis of Seismicity in Iran. *Pure Appl Geophys* 2017;174:793–833. <https://doi.org/10.1007/s00024-016-1435-4>.
- [32] Mousavi-Bafrouei SH, Mahani AB. A comprehensive earthquake catalogue for the Iranian Plateau (400 B.C. to December 31, 2018). *J Seismol* 2020;24:709–24. <https://doi.org/10.1007/s10950-020-09923-6>.
- [33] Savidge E, Nissen E, Nemati M, Karasözen E, Hollingsworth J, Talebian M, et al. The December 2017 Hojedk (Iran) earthquake triplet—sequential rupture of shallow reverse faults in a strike-slip restraining bend. *Geophys J Int* 2019;217:909–25. <https://doi.org/10.1093/gji/ggz053>.
- [34] Talebi M, Sivandi-Pour A, Ahmadi G-A, Farsangi EN, Esmaeili S, Banimahdi-Dehkordi M-J, et al. A reappraisal of active faults in central-east Iran (Kerman province). *Earthq Sci* 2022;35:122–37. <https://doi.org/10.1016/j.eqs.2022.05.001>.
- [35] Gutiérrez F, Ilyati I, Rezaei M, Zarei M, Hudec M. Active strike-slip faulting, diapirism and seismic hazards. The case of the Kareh Bas fault and the associated Dandenjan salt extrusion in the Zagros Mountains, SW Iran. *J Struct Geol* 2024;187:105239. <https://doi.org/10.1016/j.jsg.2024.105239>.
- [36] Amini Hosseini K, Hosseini M, Izadkhah YO, Mansouri B, Shaw T. Main challenges on community-based approaches in earthquake risk reduction: Case study of Tehran, Iran. *Int J Disaster Risk Reduct* 2014;8:114–24. <https://doi.org/10.1016/j.ijdrr.2014.03.001>.
- [37] Community based activities in Tehran. Tehran, Iran: Tehran Disaster Mitigation and Management Organization 2007.
- [38] Karimiparidari S, Zaré M, Memarian H. New seismotectonic zoning map of Iran. *Proc. 6th Int. Conf. Seismol. Earthq. Eng.*, 2011. <https://www.bhrc.ac.ir/en> n.d.
- [39] <https://www.bhrc.ac.ir/en> n.d.
- [40] Iwata D, Nanjo KZ. Adaptive estimation of the Gutenberg–Richter b value using a state space model and particle filtering. *Sci Rep* 2024;14:4630. <https://doi.org/10.1038/s41598-024-54576-x>.
- [41] Bhattacharyya P, Chatterjee A, Chakrabarti BK. A common mode of origin of power laws in models of market and earthquake. *Phys A Stat Mech Its Appl* 2007;381:377–82. <https://doi.org/10.1016/j.physa.2007.02.096>.
- [42] Gutenberg B, Richter C. *Seismicity of the earth and associated phenomena*. Princeton University Press; 1954.
- [43] Dubiński J, Stec K, Krupanek J. Comprehensive use of the Gutenberg–Richter law and geotomography for improving seismic hazard evaluation in hard coal mines. *Int J Coal Sci Technol* 2023;10:3. <https://doi.org/10.1007/s40789-022-00561-6>.
- [44] Main IG, Al-Kindy F. Reply to “Comment on ‘Entropy, energy, and proximity to criticality in global earthquake populations’” by Chien-chih Chen and Chun-Ling Chang. *Geophys Res Lett* 2004;31. <https://doi.org/10.1029/2004GL019497>.
- [45] Cirella A, Piatanesi A, Cocco M, Tinti E, Scognamiglio L, Michelini A, et al. Rupture history of the 2009 L’Aquila (Italy) earthquake from non-linear joint inversion of strong motion and GPS data. *Geophys Res Lett* 2009;36. <https://doi.org/10.1029/2009GL039795>.
- [46] Pisarenko VF, Sornette D. Characterization of the Frequency of Extreme Earthquake Events by the Generalized Pareto Distribution. *Pure Appl Geophys* 2003;160:2343–64. <https://doi.org/10.1007/s00024-003-2397-x>.
- [47] Huang H-H, Wu Y-M, Song X, Chang C-H, Lee S-J, Chang T-M, et al. Joint Vp and Vs tomography of Taiwan: Implications for subduction-collision orogeny. *Earth Planet Sci Lett* 2014;392:177–91. <https://doi.org/10.1016/j.epsl.2014.02.026>.
- [48] Mazandarani A, Mahlia TMI, Chong WT, Moghavvemi M. A review on the pattern of electricity generation and emission in Iran from 1967 to 2008. *Renew Sustain Energy Rev* 2010;14:1814–29. <https://doi.org/10.1016/j.rser.2010.03.014>.
- [49] Iran IR: Electric Power Consumption: per Capita, <https://www.ceicdata.com/en>. <https://www.ceicdata.com/en/iran/energy-production-and-consumption/ir-electric-power-consumption-per-capita..>
- [50] Iran Electricity Production, <https://www.ceicdata.com/en>. <https://www.ceicdata.com/en/indicator/iran/electricity-production#:~:text=Key%20information%20about%20Iran%20Electricity,Mar%201964%20to%20Mar%202023..>
- [51] Iran Energy Information, [https://www.enerdata.net/Estore/Energy-Market/Iran/#:~:text=Iran%20Power%20Consumption,%2C%20and%20services%20\(19%25\).](https://www.enerdata.net/Estore/Energy-Market/Iran/#:~:text=Iran%20Power%20Consumption,%2C%20and%20services%20(19%25).)
- [52] <https://www.murata.com/>.